ROYAL SOCIETY
OF CHEMISTRY

REVIEW

Check for updates

Liquid crystal polymer actuators with complex and multiple actuations

Xiaoyu Zhang, [ID] Jia Wei, [ID] * Lang Qin [ID] * and Yanlei Yu [ID]

Deformable liquid crystal polymers (LCPs), which exhibit both entropic elasticity of polymer networks and anisotropic properties originating from ordered mesogens, have gained more and more interest for use as biomedical soft actuators. Especially, LCP actuators with controllable mesogen alignment, sophisticated geometry and reprogrammability are a rising star on the horizon of soft actuators, since they enable complex and multiple actuations. This review focuses on two topics: (1) the regulation of mesogen alignment and geometry of LCP actuators for complex actuations; (2) newly designed reprogrammable LCP materials for multiple actuations. First, basic actuation mechanisms are briefly introduced. Then, LCP actuators with complex actuations are demonstrated. Special attention is devoted to the improvement of fabrication methods, which profoundly influence the available complexity of the mesogen alignment and geometry. Subsequently, reprogrammable LCP actuators featuring dynamic networks or shape memory effects are discussed, with an emphasis on their multiple actuations. Finally, perspectives on the current challenges and potential development trends toward more intelligent LCP actuators are discussed, which may shed light on future investigations in this field.

1. Introduction

Intelligent soft materials, such as liquid crystal polymers (LCPs), hydrogels, and shape memory polymers (SMPs), have attracted great interest due to their excellent external

Department of Materials Science & State Key Laboratory of Molecular Engineering of Polymers, Fudan University, Shanghai, 200433, China.
E-mail: weijia@fudan.edu.cn, qinlang@fudan.edu.cn, ylyu@fudan.edu.cn

stimulus responsiveness and adaptability to changing environments.[1–4] Such materials exhibit huge potential to facilitate the development of intelligent actuators in biomedical engineering, since they possess superior compatibility and affinity to living organisms.[5,6] To extend the self-adaptive behaviours and functionalities of actuators in the corresponding applications, much effort was made to develop soft materials that demonstrate tunable stimuli-induced responses.

Xiaoyu Zhang

Xiaoyu Zhang is currently a PhD student at the Department of Materials Science, Fudan University (China). She received her BS degree from the College of Polymer Science and Engineering at Sichuan University (China) in 2021. Her research interests focus on the design of liquid crystal polymers and soft actuators.

Jia Wei

Jia Wei is an associate professor in the Department of Materials Science at Fudan University, China. She received her BS degree in applied chemistry from East China University of Science and Technology in 1999, obtained her MS degree in polymer physics and chemistry from East China Normal University in 2002 and PhD from Fudan University in 2005. Since then, she has been working at Fudan University. During 2008–2011, she was a research fellow in School of Materials Engineering Science and Technology at Nanyang Technological University. Her research interests are focused on the innovative design and synthesis of photoresponsive polymers.

This journal is © The Royal Society of Chemistry 2024

J. Mater. Chem. B, 2024, **12**, 6757–6773 | **6757**

LCPs are desirable property-tunable soft materials, which possess both the anisotropy of liquid crystals (LCs) and the entropy elasticity of polymers. Especially, LCPs with ordered mesogen alignment and crosslinked networks stand out among intelligent materials for soft actuator applications because they perform large amplitude and reversible anisotropic deformation under external stimulus.[7–10] For example, a typical LCP strip enables the lifting of a weight over 1000 times of its own, with a specific work capacity of around 50 J kg^{-1}, which are comparable to the behaviors of human muscle tissues.[11] Beyond pursuing LCP actuators with better deformability for simple contraction/expansion, scientists have also made great efforts in the development of complex actuations, such as bending, curling, twisting, oscillating, and out-of-plane actuation, to obtain more sophisticated functions for practical applications.[12–15]

Up to date, LCP actuators with complex actuations have been mainly constructed through two kinds of strategies: the first is aligning the mesogens in a patterned manner to create inhomogeneity of the alignment; the second is fabricating aligned LCP actuators with 3D geometries to generate inhomogeneity of structures. However, the typical patterned aligning techniques, which require surface anchoring, usually restrain the preparation of LCP actuators in the LC cells and result in a 2D film. Besides, linear LCPs, which allow the construction of aligned 3D actuators due to the self-assembly capacity, are inapplicable to the patterned aligning techniques that depend on the anchoring effect. Therefore, it has remained a challenge for a long time to realize a patterned alignment and 3D geometry simultaneously in a monolithic LCP actuator, though their combination is obviously conducive to the further development of complex actuations. The most critical obstacle that impedes the combination is the absence of an appropriate fabrication method, which ensures the local control of the alignment and geometry of LCP actuators as desired. Recently, the ingenious utilization of 3D printing opens a door to the fabrication of LCP actuators with complex actuations.[16] 3D printing is widely acknowledged as a powerful additive manufacturing technology for constructing complex 3D objects in a layer-wise manner. More notably, the external force generated during the extrusion process of printing aligns the mesogens effectively. By adjusting the printing paths and parameters with the assistance of computer-aided design, both the mesogen alignment and the geometry are regulated. Accordingly, 3D printing exhibits great potential to increase the complexity and promote the diversity of the actuation modes of LCP actuators, which is critical for the creation of really usable LCP actuators.

In a real usage scenario, the working environment for actuators is usually changeable. However, most reported LCP actuators only possess single actuation mode, and are commonly used in a stable working environment. To further broaden the applications of LCP actuators, it is critical to endow the LCP actuators with multiple actuations for handling variable surroundings.[17–20] The studies focusing on LCP actuators with multiple actuations are at the rising stage, and ever-more inspiring works have been reported recently. For LCP actuators, the change of geometry or the change of the mesogen alignment will make for a different actuation mode. Accordingly, LCP actuators with multiple actuations become achievable through the creation of reprogrammable LCP materials, which allow the reprogramming of the geometry and even the mesogen alignment. The most widely used method for the endowment of reprogrammability is the combination of dynamic networks and LCP materials, while the integration of the shape memory effect and LCP materials appears to be another newlydeveloped but promising method. The innovation of reprogrammable LCP materials gives scientists a chance to get a step closer to actuators as found in nature, which adapt changing environments through selective exhibition of multiple attainable actuations.

Here, we provide a brief overview of the development and the cutting edge of LCP actuators (Fig. 1). The basic mechanisms of
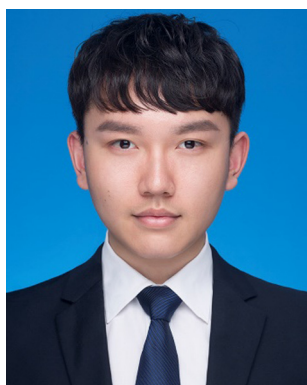
Lang Qin is an associate research fellow in the Department of Materials Science at Fudan University (China). He received his BS degree in materials chemistry from Sun Yat-sen University (China) in 2013 and received his PhD degree in materials physics and chemistry from Fudan University (China) in 2018. He continued his research in Fudan University as a postdoctoral research fellow. His research interests focus on the design of functional liquid crystal materials and the construction of photonic crystals.

Lang Qin

Yanlei Yu is a professor in the Department of Materials Science at Fudan University, China. She graduated in applied chemistry from Anhui University in 1993 and obtained her MS degree in polymer chemistry and physics from the University of Science and Technology of China in 1996. She obtained her PhD degree in environmental chemistry and engineering from Tokyo Institute of Technology and was promoted to a full professor at Fudan University in 2004. Her research interests focus on the development of photodeformable smart materials and liquid crystal polymers.
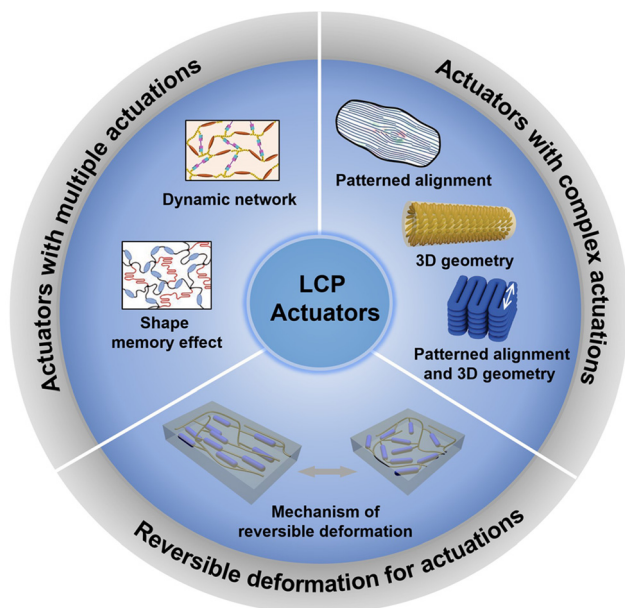
Yanlei Yu

Fig. 1 LCP actuators with complex and multiple actuations.

Fig. 2 (a) A schematic illustration showing the mechanism of the reversible stimulus–response deformation of crosslinked LCPs. (b) A schematic illustration showing the phase transition driven by heat. (c) A schematic illustration showing the phase transition driven by light, with the orange rods representing the *trans* isomers and the red bent-structures representing the *cis* isomers.

reversible deformations and aligning techniques of LCP actuators are presented at the beginning. Afterwards, diverse LCP actuators with complex actuations are introduced, and special attention is devoted on the fabrication methods for tailoring the mesogen alignment and geometry. Then, the LCP actuators with multiple actuations are shown, with the design of reprogrammable LCP materials being highlighted. Within this framework, we provide an outlook for higher intelligence of the LCP actuators enabled by complex and multiple actuations in the near future, following the trend of material demands and fabrication method requirements.

2. Actuation mechanisms of LCP actuators

2.1 Mechanisms of reversible deformation of LCP actuators

Generally, reversible stimulus-response deformation of LCPs requires both macroscopic ordered mesogen alignment and crosslinked networks. As shown in Fig. 2a, under certain external stimulus (heat, light, electric, magnetic, *etc.*), the ordered alignment of mesogens is disrupted as a result of phase transition.[21–31] Since the mesogen alignment is interconnected with the conformation of the polymer backbone, the macroscopic deformation of the crosslinked LCPs is achieved through the amplification of the microscopic change of the mesogen alignment. Besides, the initial orientation of the mesogens is fixed by the crosslinked network, so the mesogens rearrange to an ordered structure and the deformed crosslinked LCPs return to their original shape, when the phase recovers from the isotropic to LC phase. The alignment-dependent shape change behavior of the crosslinked LCPs is reversible and repeatable, which makes them suitable for the use of actuator applications.
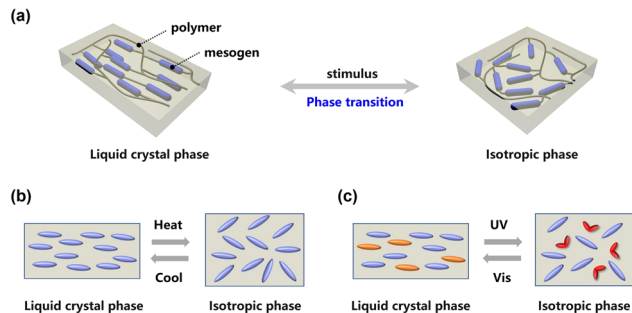
By far, the most common stimulus for triggering the phase transition of LCP actuators is heat (Fig. 2b). When heated above the nematic-to-isotropic temperature (T_{NI}), the phase of LCP actuators transits from the LC to isotropic phase and the ordered mesogen alignment is interrupted. When cooled below T_{NI}, the phase of LCP actuators recovers to the LC phase and the mesogens align in order again. Another widely used stimulus for triggering the phase transition is light, which attracts numerous research interests due to its capacities of remote, tunable and precise control. Generally, researchers endow the LCPs with light-responsive properties by incorporating photothermal molecules for photothermal effects or photosensitive molecules for photochemical reactions. For the LCPs with photothermal molecules, the temperature of LCPs is heated above T_{NI} under the irradiation of light by converting the light into heat, which induces the phase transition in terms of the same mechanism as the thermally induced one. For the LCPs with photosensitive molecules (Fig. 2c), the typical photochemical phase transition is driven by *trans–cis* isomerization of azobenzene mesogens. Azobenzene mesogens have two isomeric states: a rod-like *trans* configuration that stabilizes ordered mesogen alignment, and a bent-shape *cis* isomer that tends to destabilize the mesogen alignment. The *trans–cis* isomerization of azobenzene is usually induced by UV light irradiation, which disrupts the alignment of azobenzene mesogens in the irradiated area. Due to the cooperative effect in LC molecules, the alignment changes of only 1 mol% of azobenzene mesogens in response to light are enough to change the alignment of the whole system. Thereby, the phase transition is triggered isothermally by the photochemical reaction under the irradiation of light. Through the thermal relaxation or visible-light irradiation, the phase of LCPs returns to the initial LC phase *via* the *cis*-to-*trans* isomerization.[12,32,33]

2.2 Mechanisms of aligning techniques of LCP actuators

The crosslinked LCPs with aligned mesogens are mainly fabricated *via* two steps: (1) aligning mesogens (in the original monomer, oligomer, or weakly crosslinked polymer); (2) forming a crosslinked network for locking the oriented mesogens

This journal is © The Royal Society of Chemistry 2024

J. Mater. Chem. B, 2024, **12**, 6757–6773 | **6759**

and the obtained geometries. Since the mesogen alignment determines the deformation mode of the LCP actuator in certain geometry, the aligning techniques for controlling the orientation direction has been the center of attention of many studies. Hitherto, the two most widely used techniques for aligning mesogens are mechanical alignment in the two-step crosslinked method proposed by Finkelmann, and surface alignment in the one-step crosslinked method reported by Broer.[26,34]

The mechanical alignment is universally applied to polysiloxane-based LCPs, which allow the uniform uniaxial alignment up to the centimeter scale. Fig. 3a shows how mechanical alignment works in the classical two-step crosslinked method. The method starts with a linear, nonfunctional polyhydrosiloxane chain, which is coupled with the mesogenic groups and crosslinkers. In the first step, the vinyl groups react very fast, leading to a weakly crosslinked network. This network is deformed with a constant load to induce the network anisotropy, and then the mesogens are aligned along the direction of the external force. In the second step, the slower reaction of the methacrylate groups leads to a full crosslinked network, which locks the uniaxial alignment of the mesogens. The core requirement of the two-step crosslinked method is that the two crosslinking reactions must occur in sequence. For aforementioned polysiloxane-based LCPs, the vinyl groups react two orders of magnitude faster than methacryloyl groups according to the kinetic studies.[14,26] The time difference between the two reactions makes it possible for polysiloxane-based LCPs to form crosslinked networks sequentially. Generally, the LCP actuators fabricated as mentioned above are usually uniaxially oriented strip-shaped actuators, which usually exhibit reversible contraction and expansion upon stimulus.

Another newly developed two-step crosslinked method realizes the sequential formation of crosslinked networks through orthogonal stimuli for triggering the reactions. In the first step, the aza/thiol-Michael (acrylate) step growth polymerization for the weakly crosslinked network is initiated by heat. In the second step, the free radical polymerization for the fully crosslinked network is driven by light. Therefore, the newly developed method is a non-time dependent process because of the distinct stimuli, and the convenient aza/thiol-Michael addition makes it easy to prepare the weakly crosslinked LC network. These characteristics of this method attract wide research interests and provide the opportunities for 3D printing technologies to be used in the fabrication of LCP actuators.[35–37]

The surface alignment is usually applied to polyacrylate-based LCPs, which allow various orientation types of mesogens such as homogeneous, homeotropic, splay and twist.[14,15,34,38–44] Fig. 3b shows how surface alignment works in the classical one-step crosslinked method. Firstly, the LC and crosslinkers are thoroughly mixed, and then the capillary action is employed to introduce the mixture into the LC cell. Then, the LC diacrylates align in an ordered manner due to the anchoring effect of the alignment layer. Subsequently, the free-radical polymerization is initiated by an external stimulus to form a crosslinked network, according to which the mesogen alignment is fixed.

Generally, LC cells consist of spacers and two glass substrates coated with alignment layers. It is worth noting that the alignment layers are the key components of the LC cells, because the surface morphology and physicochemical properties of which determine the orientation types of mesogens. The alignment layers are typically made of polyimide (PI), which is treated with friction rubbing to obtain directional grooves. Through the interactions between the mesogens and the grooved surface of alignment layers, the mesogens are aligned along the axial direction of the grooves. Another kind of commonly used alignment layers is PI coated with alignment agents, and the mesogens are aligned vertical to the glass substrates due to the physicochemical effect.

By employing the same alignment layers, two main orientation types, homogeneous and homeotropic orientations, are obtained. Furthermore, the splay orientation is achieved via the combination of one homogeneous alignment layer and one homeotropic alignment layer, and the twist orientation is realized through the addition of chiral molecules. Designable regulation of mesogen alignment promotes the realization of LCP actuators with various actuation modes, such as contraction/expansion, bending/unbending, winding/unwinding and even continuous waving.[45,46] Nevertheless, LCP actuators fabricated as mentioned above are usually restrained in 2D thin film geometry, because the effective depth of the anchoring effect is limited to the micrometer scale and the actuators need to be shaped in LC cells.

Subjected to the characteristics of these aligning techniques, most reported LCP actuators exhibit simple alignment and geometry. However, it is significant to increase the complexity of the actuations as the practical applications require. Thereby, creating LCP actuators with complex actuations has become a research hotspot in these years.

Fig. 3 (a) General schematic of two-step crosslinked method applying mechanical alignment. Reproduced with permission from ref. 26. Copyright 2022 Wiley-VCH. (b) General schematic of one-step crosslinked method applying surface alignment.

3. LCP actuators with complex actuations

Substantially, controlling the mesogen alignment in a patterned manner and endowing the aligned LCP actuators with
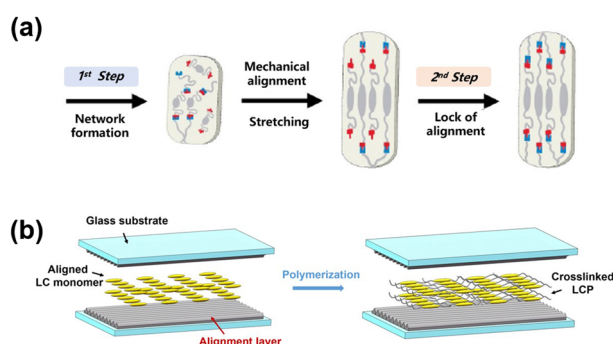
3D geometry are both effective strategies for constructing LCP actuators which perform complex multi-dimensional actuations. Up to date, researchers have developed patterned alignment layers for the precise local control of mesogen alignment, and linear LCP materials for the fabrication of LCP actuators with 3D geometry. Nevertheless, LCP actuators aligned by patterned alignment layers are usually restrained in geometry of 2D films. 3D LCP actuators which are made by linear LCP materials, on the other hand, are incompatible with patterned aligning techniques based on alignment layers. So, how to combine the patterned mesogen alignment and 3D geometry in the same monolithic actuator has remained a challenge for a long time. Breakthrough of this bottleneck problem is the utilization of 3D printing in the fabrication of LCP actuators. During the 3D printing process, the 3D geometry is constructed by the layer-wise additive manufacturing, and the mesogens are arranged in a patterned manner through the design of the printing path. Accordingly, LCP actuators with both patterned mesogen alignment and 3D geometry are fabricated *via* 3D printing, which exhibit more sophisticated actuations.

3.1 Complex deformation of 2D films with patterned orientation

To obtain a patterned orientation, the construction of patterned alignment layers provides an effective way for the LCP actuators fabricated based on the one-step crosslinking method, since the surface morphology and physicochemical properties of alignment layers determine the mesogen alignment.[23,47–49] In general, the patterned alignment layers can be realized by aligning photosensitive molecules, usually azobenzene-containing materials, with polarized light (Fig. 4a) or patterning topographical features with lithography (Fig. 4e).

Photoalignment is proven to be an attractive method for preparing patterned alignment layers, and depends on the Weigert effect or the photo-reorientation of azobenzene-containing alignment agents in response to linearly polarized light. Under the irradiation of linearly polarized light, the *trans*-azobenzene molecules perpendicular to the polarization direction do not absorb light and keep stable, while the molecules aligned in other directions absorb energy into an excited state, and then undergo *trans–cis* isomerization. After repeated *trans–cis–trans* isomerization cycles, all the azobenzene molecules will be perpendicular to the polarization direction of light. That is to say, the molecular directions of the alignment layers can be customized by the polarization direction of light, thus ensuring the molecules arranged in a patterned manner benefiting from the accurate local control of light. In a glass cell with photoalignment layers, the mesogens will be aligned along the direction of the photoaligned molecule due to the molecular interactions, thereby being encoded with patterned orientation.

Broer *et al.* invented a straightforward method for engineering patterned alignment layers with photoalignment.[47] As shown in Fig. 4a, by slowly rotating the cell while irradiating through a photomask with a wedge-shaped opening, cells coated with the alignment material formed a patterned alignment layer

accordingly, which in turn induced the complex patterned orientation of mesogens. Due to the ability of linearly polarized light to rotate 360° within the plane, this orientation method offered extremely high precision, making it highly valuable for preparing LCPs capable of achieving complex deformations. With this method, Broer *et al.* prepared IR-responsive LCP films with patterned orientations (Fig. 4b) capable of performing complex actuations. In the case of an azimuthal alignment pattern, a reduction of the liquid crystal order upon temperature increase led to compression along the azimuthal direction and an expansion along the radial direction. These stresses were not able to be accommodated within the sheet plane, causing the deformation of the flat sheet out of the plane into a cone. In the case of a radial alignment pattern, the opposite deformations took place. This resulted in an anti-cone, which was recognizable as a saddle shape.

Afterward, White *et al.* further improved the accuracy of photoalignment by replacing the photomask with a cylindrical lens, which was used to focus the expanded laser beam into a sharp line (<50 μm width, 1.6 cm length).[48] Benefitting from the improved accurate fabrication technique of alignment layers, White *et al.* realized patterned orientation in azobenzene-containing films with defects ranging from $-5/2$ to $+5/2$ (Fig. 4c). By varying the ratio of the polarization rotation rate, R_1, to the sample rotation rate, R_2, different defect strengths were regulated for diverse topographical transformation. Later on, they realized doubly precise local control towards the orientation director of LCPs by improving the sensitivity of the LCP materials to the surface alignment. By combining the large strain inherent to LCPs, the sensitivity of the materials chemistry to surface alignment, and the optical patterning methods, a voxelated LCP containing nine defects in a square array was achieved (Fig. 4d) whose director was written within local volume elements (voxels) as small as 0.0005 cubic millimeters.[23] Remarkably, macroscopic azimuthal contraction along the director and radial expansion around each defect center led to the emergence of cones centering on each $+1$ defect, demonstrating exquisite deformation behavior based on the precise imprinting of topological defects in LCPs.

Another effective method for preparing patterned alignment layers is based on the combination of the laser direct writing technique and replica molding reported by Yang *et al.*[49] As shown in Fig. 4e, masters with 1D channels were fabricated from photoresist using direct laser writing at first, after that, a PDMS mold was replicated from the master. To create 1D channels with surface anchoring to align mesogens, the PDMS mold was replicated to the epoxy mold. Accordingly, an even smaller pattern feature size of 1 μm that gives a much higher surface anchoring energy was prepared, enabling the control of the arbitrary position-dependent orientation of the mesogens.

Based on the alignment layers ensuring local accurate control of mesogen alignment as desired and a numerical algorithm, they demonstrated reversible deformation from the flat sheet to an intricate 3D geometry. The author adopted an oxygen-mediated thiol-acrylate "click" reaction instead of traditional LCP photopolymerization chemistry to lock the LC
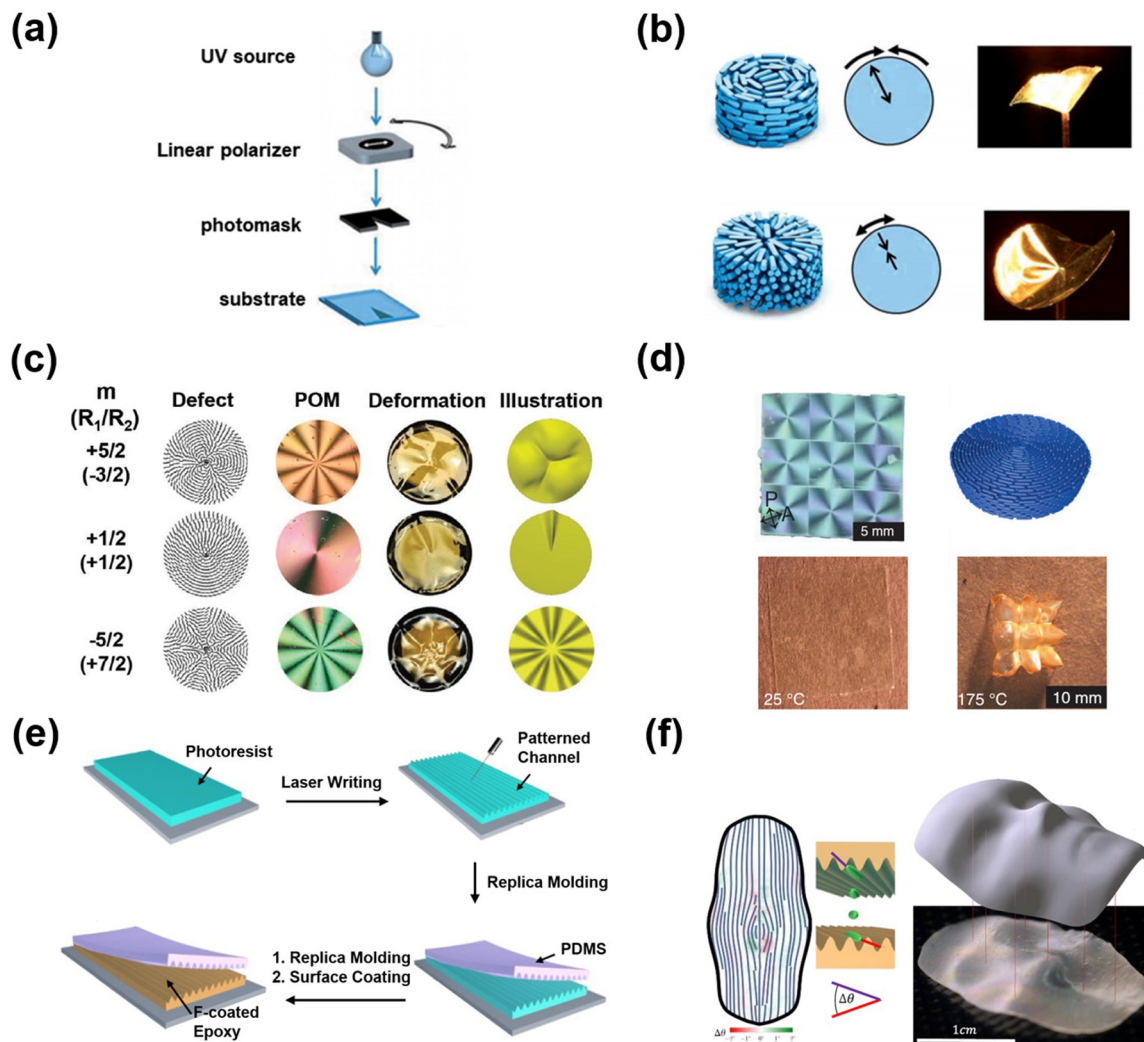
Fig. 4 (a) The setup for the preparation of patterned alignment layers based on the polarized light. (b) Actuation of films with azimuthal and radial alignments. Reproduced with permission from ref. 47. Copyright 2012 Wiley-VCH. (c) Summary of the director field, polarized optical microscopy image, photomechanical response of film and illustration of photomechanical response for azo-LCP films subsumed with topological defects ranging from −5/2 to +5/2. Reproduced with permission from ref. 48. Copyright 2013 Wiley-VCH. (d) The pixel level liquid crystal orientation control and the corresponding reversible conical deformation. Reproduced with permission from ref. 23. Copyright 2015 AAAS. (e) The fabrication procedure of patterned alignment layers based on laser direct writing and replica molding. (f) Two slightly different director fields are imposed on the top and bottom surfaces of the LCE sheet. At the target temperature 180 °C, the LCP sheet takes the shape of a face. Reproduced with permission from ref. 49. Copyright 2019 American Wiley-VCH.

director field in the local domains, preventing nonuniform crosslinking density across the film. Then with the aid of a patterned alignment layer, both the arbitrary position-dependent orientation and the magnitude of local principal strains throughout the film can be precisely controlled. Based on the advancement in material systems and patterned alignment layers, spatially heterogeneous LCPs with lateral deformation at every point working as designed by the algorithm were prepared, achieving the deformation from a flat sheet to the preferred intricate isometry – a face (Fig. 4f). Apart from the aligning techniques mentioned above, applying magnetic field is also an effective method for the patterned alignment in 2D films.[14] For example, Zentel et al. have achieved radically aligned LCP actuators with a radically symmetric magnetic

field, which exhibited circularly symmetric actuation similar to iris.[50]

3.2 3D actuators constructed by self-assembled linear LCPs

Compared with the patterned alignment which achieves complex actuations by providing inhomogeneity of orientation, endowing the LCP actuators with 3D geometry achieves it from another perspective of offering the inhomogeneity of spatial structures. Affected by the processing conditions, typical actuators fabricated either by a one-step or a two-step crosslinking method are limited in simple geometries such as 2D films or strips. To shape the aligned LCP actuators into complex structures beyond films or strips, researchers have attempted to utilize the replica molding for the construction of

6762 | J. Mater. Chem. B, 2024, 12, 6757–6773

This journal is © The Royal Society of Chemistry 2024

microstructured LCP actuators, with the magnetic field inducing uniaxially aligned mesogens at the same time.[51–53] Keller *et al.*, for instance, have realized LCP actuators with the geometry of micrometer-sized array pillars, which demonstrated ultralarge and reversible contractions compared to the macroscopic systems reported in the literature.[54] Breakthroughs of the construction of even more complicated 3D geometry were anticipated by developing novel linear LCP (LLCP) materials, which possessed improved processibility compatible with commonly used polymer processing methods.[55–57] The LLCPs possess self-assembly capacity, ensuring the mesogens to be aligned by annealing even after the shaping of actuators, thus realizing the construction of aligned 3D LCP actuators.

In 2016, Yu *et al.* synthesized a LLCP using the ring-opening metathesis polymerization (ROMP) method for the fabrication of 3D actuators.[55] As shown in Fig. 5a, the LLCP synthesized *via* ROMP exhibited high-molecular-weight, which not only enhanced the mechanical properties but also offered the chain entanglement as physical crosslinking. Furthermore, the flexible main chain and long spacer groups of the LLCP provided sufficient free volume. Accordingly, the azobenzene mesogens self-assembled into a well-ordered layered structure (Fig. 5b), with the mesogens tilted at an angle of $\phi = 65°$ in the lamellar layers when annealing. Due to the ordered lamellar structure and high molecular weight, the LLCP was strong and tough as well as possessed an effective physical crosslinked network, which ensured the reversibility of deformation and the compatibility for commonly used polymer processing methods.

Liberated from the constraints of aligning methods such as mechanical stretching or surface alignment towards the geometries of actuators, the self-assembly ability of the mesogens in the LLCP decoupled the formation of geometries and the aligning process for the fabrication of aligned LCPs.
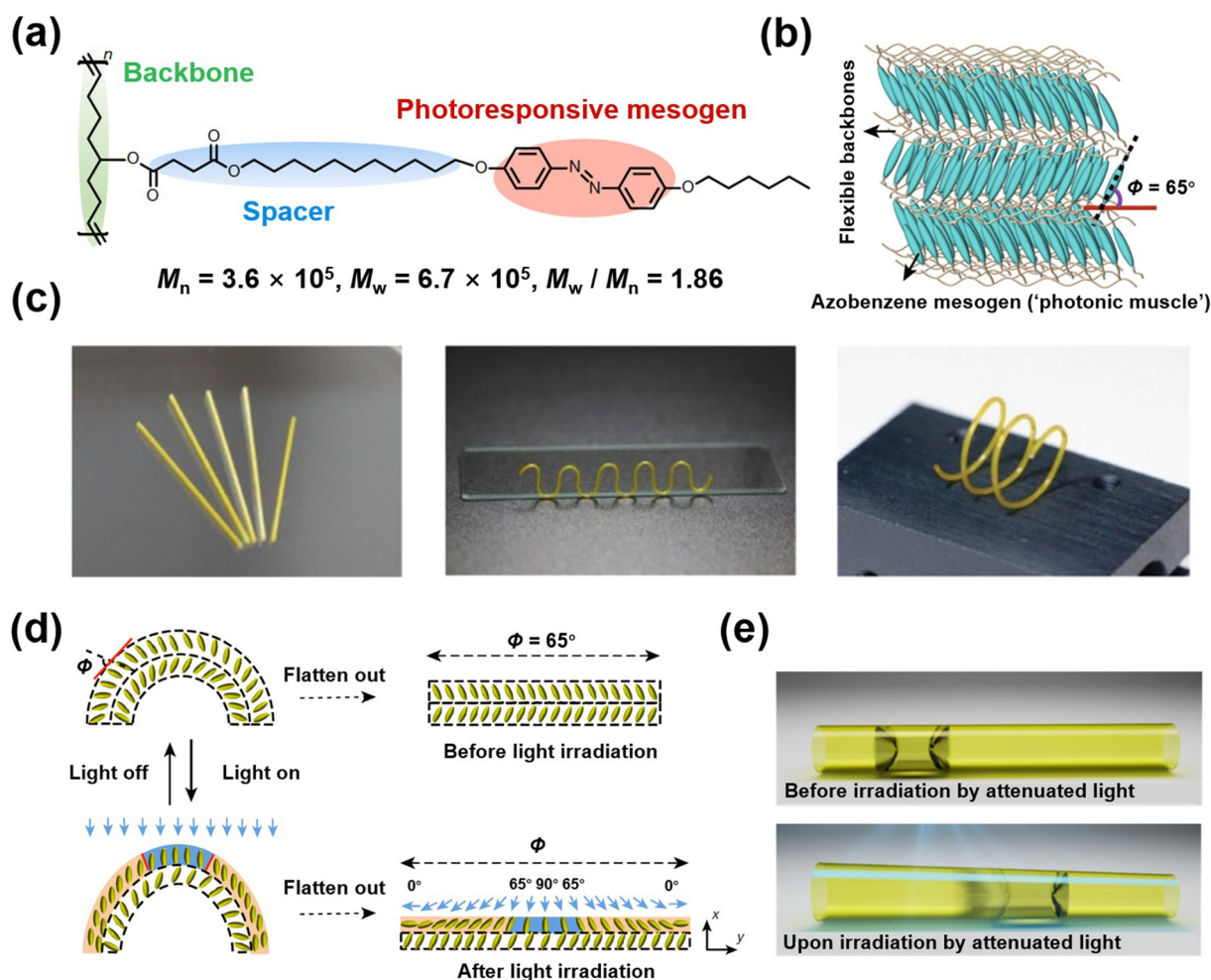

Fig. 5 (a) Molecular structure of a novel linear liquid crystal polymer (LLCP). M_n, number-average molecular weight; M_w, weight-average molecular weight. (b) Schematic representation of the packing structure in the LLCP film. ϕ denotes the tilt angle between the long axis of the azobenzene mesogens and the plane of the lamella. (c) Photographs showing left to right a batch of free-standing straight, serpentine and helical TMAs. (d) Schematic illustration showing the mechanism of the deformation of the TMA before and after irradiation by unpolarized 470 nm light in the cross-sectional area. To facilitate understanding of the photo-reorientation, the wall is flattened out into a plane. The normal direction of the lamellae is along the x direction in the scheme. (e) Schematics showing the motion of a slug of fully wetting liquid confined in a tubular micro-actuator driven by photodeformation.

This journal is © The Royal Society of Chemistry 2024

J. Mater. Chem. B, 2024, **12**, 6757–6773 | **6763**

Accordingly, a series of tubular micro actuators (TMAs) using melt or solution processing were obtained (Fig. 5c). When the TMAs were exposed to unpolarized 470 nm light whose actinic direction is perpendicular to the long axis of the TMAs, the azobenzene mesogens were reoriented along the propagation direction (Fig. 5d). Therefore, the tilt angle ϕ of azobenzen mesogens in the different exposed areas were different because the lamellae of the LLCP were arranged coaxially in the TMA wall. In order to facilitate understanding of this photo-reorientation, the wall of the TMA was flattened out into a plane. Calculated from 2D WAXD, under irradiation, the azo-benzene mesogens in ~70% of the exposed area were reoriented to exhibit $\phi \leq 65°$, which means that this area expanded along the y axis. The rest of the azobenzene mesogens were tilted with $65° < \phi \leq 90°$, leading to a contraction along the y axis. Therefore, the light-exposed area demonstrated expansion overall, causing an increase of the cross-sectional area of the TMA. Since the higher light intensity contributed to the larger increase of the cross-sectional area, the TMA deformed to an asymmetric cone-like geometry upon irradiation of attenuated 470 nm light (Fig. 5e), generating adjustable capillary force to propel liquids in the direction of light attenuation and showing huge potential for application in actuators for biomedical microfluidics.[58,59]

Afterwards, the authors improved the photodeformation properties and mechanical properties by varying the spacer length.[60] With the increasing spacer length, the mesogen alignment exhibited a larger tilt angle ϕ, thus exhibiting a larger variation of mesogens in the expanded area and a smaller variation of mesogens in the contracted area for overall enhanced asymmetric photodeformation upon attenuated light. Then, the photodeformation properties were further promoted by incorporation of biphenyl mesogens.[56] Due to the high extinction coefficient of azobenzene mesogens, the light penetration depth in LLCP actuators was limited, causing only the mesogens in the shallow surface layer to undergo an alignment change upon irradiation and thus impeding the enhancement of photodeformation capacity. The incorporation of biphenyl mesogens increased the light penetration depth by reducing the proportion of azobenzene mesogens, while still maintaining the self-assembly capacity. Due to the cooperative effect of the two mesogens, the alignment change within the deeper layer was amplified to larger photodeformation.

3.3 3D actuators with patterned orientation prepared by 3D printing

LCP actuators with both sophisticated 3D geometries and locally tunable alignment are highly desirable for elevating the complexity of actuations to a higher level, however, it can be hardly achieved by the strategies mentioned above. Surprisingly, the pioneering work of applying 3D printing to LCP actuators offers new opportunities to construct LCP actuators with a pre-designed 3D architecture while controlling the local alignment of mesogens based on digital control, thus allowing inhomogeneities of both alignment and spatial geometry.[61] Among various 3D printing techniques, material extrusion

based on direct ink writing (DIW) has been most extensively investigated, which shows great compatibility with precursors of a variety of LCP systems.[62–66]

Generally, the LCP inks for 3D printing are creative oligomers synthesized *via* thiol/aza-Michael addition of mesogenic monomers and thiol/amine chain extenders with photoinitiators (Fig. 6a), wherein the reactive acrylate end groups together with the photoinitiators ensure 3D printed LCPs to crosslink upon UV exposure. In a typical fabrication process of aligned LCP actuators based on DIW (Fig. 6b), the obtained oligomer inks are first stuffed in the ink barrel. Sometimes a heater is added around the ink barrel to adjust the ink viscosity for easier extrusion. Subsequently, in the extrusion process, the inks with proper viscosities are sheared and elongated, building up mesogen alignment along the nozzle moving direction, thus ensuring local control of mesogen alignment by tuning the printing path and parameters. Afterwards, the aligned oligomer filaments are squeezed out from the nozzle and then deposited on the X–Y–Z three-axis motion-controlled printing platform. A 2D single layer is preliminarily formed in a line-by-line manner *via* depositing the extruded oligomer filaments at the designed position with controlled X–Y axis movements, and then the extruded oligomer filament is immediately photopolymerized under UV exposure to locally fix the alignment of mesogens. Finally, a pre-designed 3D geometry is fabricated in a layer-by-layer manner by controlling the Z-axis motion of either the nozzle or the printing platform.

Based on the printing strategies mentioned above, researchers have fabricated a series of aligned LCP actuators from simple to complex. For example, Lewis *et al.* printed an LCP actuator with four layers, each of which is based on equivalent Archimedean spiral print paths (Fig. 6c).[67] Using this type of print path, the LCP actuator transformed into a cone when heated above T_{NI}. As expected, the LCP actuator recovered its original dimensions and shape upon cooling. Sánchez-Somolinos *et al.* printed an auxetic re-entrant honeycomb structured LCP actuator.[68] As shown in Fig. 6c, two extremes of the actuator were fixed on a frame. Thermo-actuation of this structure led to large changes in pore shape, from re-entrant to conventional hexagonal honeycomb geometry, which was potentially useful in particle size and shape sorting devices.

Through the modeling design of DIW, patterned alignment with higher complexity can be easily manipulated.[62,67–71] Nevertheless, more sophisticated geometries such as spatial lattices are hardly achieved since the printed LCPs need to deposit on the platform or the previous layer. Accordingly, Ruike Renee Zhao and H. Jerry Qi innovatively utilized Digital Light Processing (DLP) to fabricate pre-printed supporting structures (Fig. 6d), offering a designable 3D platform for subsequent printed LCPs by DIW to deposit.[69] Benefiting from the supporting structures, the programming of the geometries of the actuators fabricated by DIW was liberated from stacking planar layers, allowing the deposition on arbitrary pre-designed points in a 3D space. To demonstrate this capability, an LCP pyramid was designed and printed. The supporting pillars with different heights were printed using the removable supporting ink by
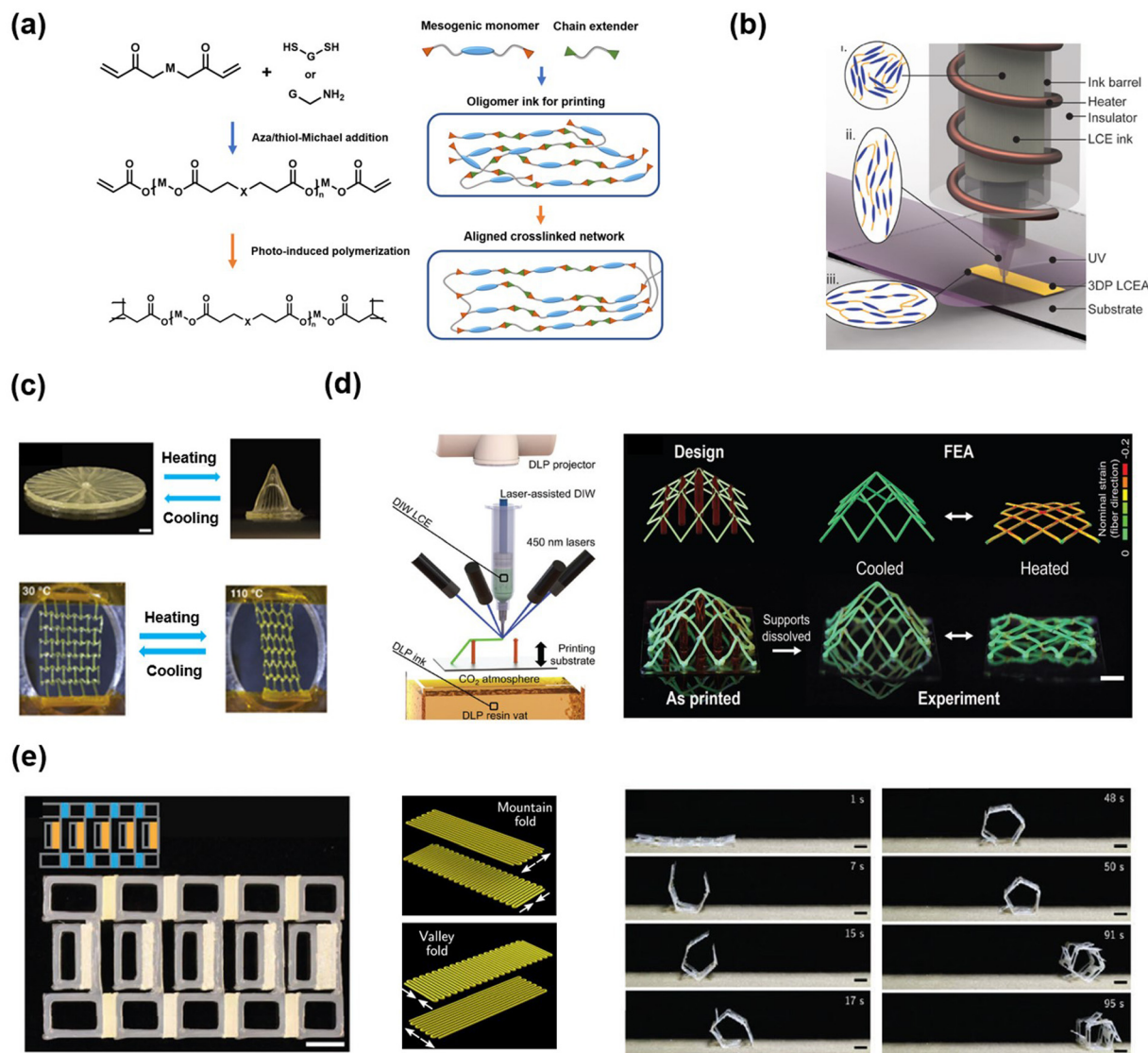
6764 | *J. Mater. Chem. B*, 2024, **12**, 6757–6773

This journal is © The Royal Society of Chemistry 2024

Fig. 6 (a) The chemical structure formula and schematic illustration demonstrating the design of LCP ink and printed crosslinked LCPs. The letter "M" represents the mesogen, the letter "G" represents a non-functional group and the letter "X" represents a thiol or amine linker. The blue rods represent mesogens, the orange triangle represents the acrylate end groups, the green triangle represents thiol/amine and the grey lines represent molecular chains. (b) Schematic illustration of HOT-DIW of the LCP ink. (c) The reversible thermal actuation of a disc-shaped LCP actuator and a honeycomb shaped LCP actuator fabricated by 3D printing. Reproduced with permission from ref. 67. Copyright 2018 Wiley-VCH. Reproduced with permission from ref. 68. Copyright 2017 Wiley-VCH. (d) Schematic of the laser-assisted hybrid DIW and DLP system as well as the design and physical photographs demonstrating the structure and actuation of the pyramid LCP actuator fabricated with this method (color represents nominal strain along the fiber direction). Reproduced with permission from ref. 69. Copyright 2022 Wiley-VCH. (e) The initial configuration of the printed self-propelling rollbot. In the legend (inset), the blue (LT_{NI}) and orange (HT_{NI}) LCP hinges denote valley and mountain folds, respectively, and gray indicates structural tiles. When heated above LT_{NI}, the printed structure folded into a pentagonal prism induced by the LT_{NI} LCP hinges. When further heated above HT_{NI}, the HT_{NI} LCP hinges propelled the rollbot, demonstrating self-propelling locomotion. Reproduced with permission from ref. 70. Copyright 2019 AAAS.

DLP. Then, the LCP filaments were knitted by DIW on the top of the pillars. After printing, the supporting pillars were removed after being dissolved in water, leaving the LCP pyramid only, which collapsed upon heating and returned to the original shape upon cooling.

Profiting from the ability to print monolithic LCP actuators with different kinds of inks, DIW offered opportunities to fabricate multi-component actuators wherein each component carried certain functions, thus allowing the actuators to perform more complex actuations in an integrated manner. For example, Lewis *et al.* created a hinged self-propelling rollbot (Fig. 6e) by designing and printing three kinds of components within the same actuator.[70] As the schematic illustration in Fig. 6e shows, the author adopted LCP inks with low T_{NI} to print LT_{NI} hinges (blue), LCP inks with high T_{NI} to print HT_{NI} hinges (orange), and non-response structural inks to print structural components, namely the tiles (gray). The HT_{NI} hinges and LT_{NI} hinges were printed in the form of $0°/90°$ and $90°/0°$ bilayers,

This journal is © The Royal Society of Chemistry 2024

J. Mater. Chem. B, 2024, **12**, 6757–6773 | **6765**

which bent into mountain and valley folds, respectively, when actuated above T_{NI}. When placed on a hotplate ($T > T_{NI}$, the temperature of the surrounding environment was higher than LT_{NI} but lower than HT_{NI}), the printed actuator exhibited self-rolling behavior. The environment temperature induced valley fold of the LT_{NI} LCP hinges, enabling the printed actuator to fold into a pentagonal prism. When in contact with the hot plate and further heated above HT_{NI}, the HT_{NI} LCP hinges actuated in a mountain fold manner as well as rolled the actuator over the adjacent vertex and onto the next hinge, which carried out the same action, propelling the self-rolling of the rollbot continuously.

Another fabrication method for 3D actuators with a patterned orientation depends on the combination of the replica molding for 3D geometry and the patterned magnetic field for aligning mesogens in an arbitrary orientation.[72,73] It is worth noting that the DIW requires mechanical processing for aligning, thereby inevitably restraining the mesogen alignment parallel to the principle symmetric axis of the filaments.[16] When it comes to the fabrication of microstructures smaller than the filaments, patterned alignment can be hardly achieved in this way. Distinct from the shearing force in DIW, the patterned magnetic field allows the mosogens to align in an arbitrary orientation even in microstructures. By combining highly controllable magnetic field with replica molding, Aizenberg *et al.* have realized patterned alignment in arrays of microposts, which performed amazing collective self-regulated deformation *via* optimized selection of the orientation director, the microstructure geometry, and the incident light.[73] Relative investigation is still in its infancy but shows considerable prospects, demonstrating potential to attract wide research interests in the future.

4. LCP actuators with multiple actuations

Departing from the mesogen alignment, the crosslinked network also plays an important role in the LCP actuators, which memorizes the original mesogen alignment and geometry. However, commonly used traditional chemical crosslinked networks impede the further diversification of both the structures and the functions of LCP actuators, because they limit the actuators in the starting geometries and initial actuation modes.

Developing reprogrammable LCP materials for actuators with multiple actuations has appeared as a promising solution. By replacing the traditional chemical networks with dynamic networks or introducing shape memory effects, the geometries and the mesogen alignments of the LCP actuators become reprogrammable. Since the mesogen alignment and geometry determine the actuation mode of the actuators, LCP actuators exhibit multiple actuation modes through their reprogramming. Obviously, the LCP actuators with multiple actuations overcome the functional boundedness of LCP actuators with only single actuation mode, and demonstrate better adaptabilities towards changeable and complex working environments.

4.1 Multiple actuations realized by dynamic networks

By introducing the dynamic networks, the geometries of LCP actuators become reprogrammable due to the rearrangement of the topological networks under external force. Furthermore, upon applying appropriate directional load, the mesogen alignment is re-aligned, with the rearranged network locking the new alignment. Both the change of the geometries and mesogen alignments alter the actuation mode of LCP actuators, so, multiple actuations are achieved by dynamic networks.

4.1.1. The mechanism of reprogramming of geometries and alignments based on dynamic networks. The evolution of the dynamic covalent bond spans a rich and extensive chronicle of scientific advancement. Especially after its combination with polymers was found to bring properties like self-healing and reprocessability, it has garnered widespread attention. Currently, researchers have reported a vast number of reversible chemical reactions, among which the most commonly used ones include the Diels–Alder reaction, ester exchange reaction, reversible exchange reactions involving disulfide or diselenide bonds, and siloxane equilibrium reaction.[20]

The geometries of polymer actuators containing dynamic covalent networks can be reprogrammed through the rearrangement of topological networks under external force (Fig. 7a)
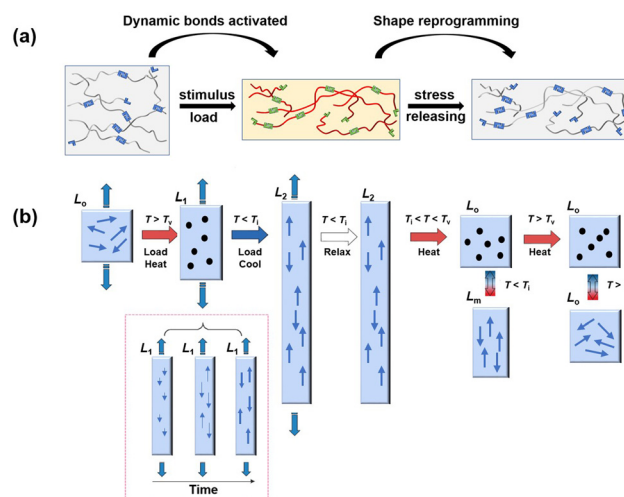

Fig. 7 (a) A schematic illustration of the shape remolding process of polymers based on the rearrangement of the topological network. Under external stimulus, the dynamic bonds are activated and the materials exhibit plasticity. Subsequently, the material in shape A is programmed into shape B, which is maintained with external force during the rearrangement of the topological network. After the inner stress stemmed from the applied force is adequately released, stable shape B can be obtained without shape change after the removal of external force. (b) Schematic illustration showing the reprogramming of LCP actuators. The original polydomain sample is heated above T_v (topology-freezing transition temperature) and then put under uniaxial stress, obtaining ordered mesogen alignment which is fixed by the rearranged network during the remolding process. Afterwards, the sample is cooled to freeze the transesterification and the load is then removed. Bringing the aligned LCP actuators into the isotropic phase (above T_{NI}), the strain energy locked by ordered liquid crystal phase is released. The final sample is remolded to a longer strip processing monodomain alignment capable of reversible deformation.

6766 | *J. Mater. Chem. B*, 2024, **12**, 6757–6773

This journal is © The Royal Society of Chemistry 2024

even after the initial crosslinked network has fully formed.[74] By introducing the dynamic networks to the LCPs, not only the geometries but also the mesogen alignment can be further re-edited. For example, Ji *et al.* introduced dynamic ester bonds in place of chemical crosslinks to LCPs, realizing re-edition of mesogen alignment, with the corresponding fundamental mechanism shown in Fig. 7b.[75] Through applying uniaxial force to the original un-oriented LCP actuator when heated above T_v (topology-freezing transition temperature) for activating the rearrangement of the dynamic network, the mesogen alignment altered from the disordered polydomain to an ordered monodomain, which was subsequently locked by the rearranged network. Afterwards, the transesterification was frozen upon cooling with the load on, memorizing the newly obtained mesogen alignment.

4.1.2. Multiple actuations based on thermally induced dynamic networks. By incorporating a diverse array of dynamic networks into LCPs, researchers have developed various LCP actuators showing distinct actuation modes before and after reprogramming due to the alteration of geometries or even the mesogen alignment. As shown in Fig. 8a, Ji *et al.* synthesized LC elastomers with exchangeable ester links (xLCEs), allowing the rearrangement of the topological network when heated above T_v ($T_{NI} < T_v$). Based on the mechanism mentioned in Fig. 8b, a free-standing monodomain xLCE strip (mode A) was reprogrammed into a spin-shaped xLCE actuator (mode B) where the mesogen alignment was induced in the walls of the pin during the high-T remolding. Accordingly, the actuation mode of the xLCE actuator changed from thermally induced contraction and elongation to reversible linear pushing force delivering.

Also based on the reversible transesterification, Ikeda *et al.* developed LCP actuators ($T_{NI} > T_v$) containing azobenzene moieties capable of performing photodeformation.[76] Through additionally introducing phenyl–OH groups in LCPs which possess high reactivity, the transesterification ensured reprogramming without the presence of catalysts. Due to T_v being lower than T_{NI}, the actuator allowed the change of only the geometry while maintaining the original mesogen alignment, without the necessity of strong external force for the inducement of ordered alignment. Accordingly, the actuator allowed the reprogramming into certain geometries beyond sharp folds, elongated strips and other similar structures for inducement of an ordered alignment. As shown in Fig. 8b, the authors remolded a monodomain oriented LCP strip (mode A) into a spiral ribbon (mode B), showing photoinduced bending and recovery in mode A while demonstrating unwinding and winding in mode B.

Subsequently, a variety of reactions based on thermally induced dynamic bonds apart from ester bonds have been applied in making LCP actuators with multiple actuations, such as transcarbamoylation and the boronic-ester exchange reaction, all of which allowed an actuator to be reprogrammed under external force at high temperature.[78,79] To further facilitate LCP actuators' reprogramming to a new height, Zhao *et al.* reported the design and study of LCP actuators with DA dynamic networks (LCDANs), allowing convenient reprogramming even at
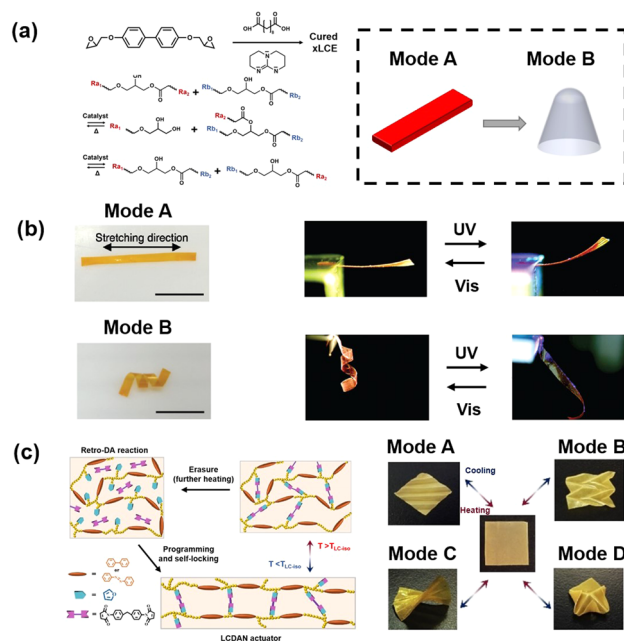

Fig. 8 (a) A schematic illustration showing the reversible transesterification of ester dynamic network and the synthesis of xLCE, with the demonstration of an aligned xLCE strip showing thermally induced contraction and elongation before reprogramming (mode A) and a spin-shaped xLCE actuator capable of delivering a linear pushing force action after reprogramming (mode B). (b) The shape reprogramming of a monodomain LCP film (mode A) into a spiral ribbon (mode B), with the exhibition of the corresponding actuation mode. Reproduced with permission from ref. 76. Copyright 2016 Wiley-VCH. (c) A schematic showing the room temperature reprogramming of LCDAN actuators based on the DA dynamic network, with the demonstration of actuators with different 3D origami architectures (mode A–D) showing thermally induced unfolding and wrinkling. Reproduced with permission from ref. 77. Copyright 2020 Wiley-VCH.

room temperature due to the mild bonding conditions of DA bonds.[77] As shown in Fig. 8c, upon heating above dissociation temperature of DA bonds, the original DA bonds broke, which needed a period of time to reform after cooling. At room temperature, the bonding kinetics were quite slow, giving the LCDAN in temporary linear status plenty of time to be oriented by applying external force. With the reformation of DA bonds over time, the mesogen alignment and the reprogrammed geometry of the obtained LCP actuators were fixed. Thanks to these brief and mild reprogramming characteristics of LCDAN, the authors easily reprogrammed the same LCDAN actuator with an initial shape of single sheets into various 3D origami structures, including accordion fold (mode A), Miura-Ori fold (mode B), Origami spiral (mode C) and Origami tent (mode D), which unfolded and refolded repeatedly on heating/cooling cycles.

4.1.3. Multiple actuations based on athermal local-controlled light-induced dynamic networks. Compared with thermally induced dynamic bonds, photoinduced dynamic bonds allow reprogramming without affecting thermotropic LC behavior because of the needlessness of heating, thus ensuring the reprogramming in a random phase. As shown in Fig. 9a, Bowman *et al.* incorporated allyl sulfides as radical-mediated
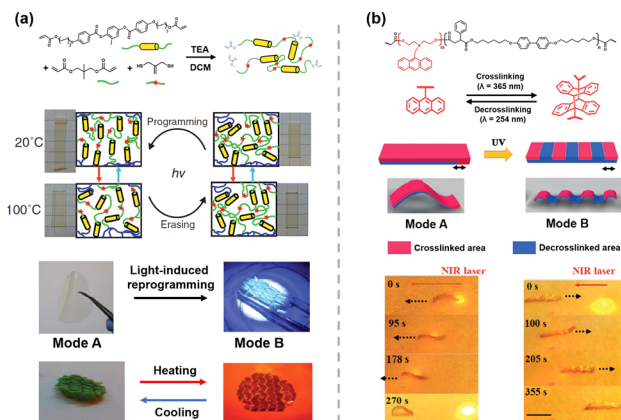
Fig. 9 (a) The synthesis route of AFT-LCPs and the schematic showing the mechanism for light-induced reprogramming, with subsequent example demonstrating reprogramming from a flat polydomain film (mode A) unable to deform into Miura fold (mode B) capable of reversible deformation. (b) Chemical structure of the anthracene-containing LCP, and the reversible photodimerization (for crosslinked) and photocleavage (for decrosslinked) of anthracene groups under UV light irradiation at two wavelengths. Subsequent schematic shows the optical reprogramming process for converting an arch-shaped light-walker into a wrinkle-shaped light-crawler through local decrosslinking, with the photographs showing the walking of the arch-shaped actuator along the laser scanning direction (from right to left) before reprogramming and the crawling of a wrinkle-shaped actuator against the laser scanning direction after programming. Reproduced with permission from ref. 81. Copyright 2019 Wiley-VCH.

addition–fragmentation chain transfer (AFT) functionalities into LCPs (AFT-LCPs), ensuring the rearrangement of the topological network triggered by light.[80] Unique to this work, by using light as the stimulus for activating the dynamic network, the rearrangement of the topological network was orthogonal to the LC phase behavior, enabling the LCPs to be reprogrammed in any LC phase or in the isotropic phase regardless of the interference brought by the change of the LC structure during the reprogramming process as their thermally induced counterparts did. Accordingly, the authors demonstrated the reprogramming of a polydomain film (mode A) unable to deform into a Miura fold (mode B) which exhibited reversible folding and flattening by simply folding the films with hands under the irradiation of UV light.

Introducing a light-induced dynamic network not only meant the decoupling between the thermotropic LC behavior and the reprogramming process, but also potentially enabled a patterned rearrangement process. Zhao *et al.* designed LCPs containing biphenyl units serving as the mesogens and anthracene pendant groups for reversible photo-crosslinking (Fig. 9b), realizing the reprogramming of an existing LCP actuator without applying external force through utilizing the local control characteristics of dynamic photo-crosslinking.[81]

The initial LCP actuator was uniaxially stretched along the direction of the black arrow shown in the schematic, and then fully crosslinked with the formation of a light-induced dynamic anthracene network, obtaining monodomain mesogen alignment. Afterwards, orientation in a certain area was erased through selective decrosslinking based on photocleavage of

the anthracene dimers, generating uneven inner stress for the alteration of geometry due to the inhomogeneity of mesogen alignment and crosslinking density. Accordingly, both the geometry and the pattern of mesogen alignment allowed reprogramming through controlling the depth and shape of the de-crosslinked area. To validate this approach, the author demonstrated the reprogramming of an arch-shaped actuator (mode A) into a wrinkle-shaped actuator (mode B) by changing the de-crosslinked area with UV irradiation, switching the walking behavior along the laser scanning direction to crawling behavior against the laser scanning direction.

It is worth noting that the introduction of dynamic bonds endows LCPs with re-programmability while sacrificing stability. The risk of actuation loss and shape distortion for LCPs with dynamic networks always existed at work and in storage, which was not satisfactory for applications that demanded creep resistance in practical environments with changing temperatures or illumination.

To address this problem, Ji *et al.* came up with a powerful but simple swelling-heating method to enable repeated switching on/off network dynamics in LCPs so as to ideally circumvent the trade-off between excellent stability and re-programmability in one single soft actuator.[20] As shown in Fig. 10a, through swelling in quenchable catalyst solution (that was, switching on), siloxane exchange was able to be induced in common siloxane LCPs for reprogramming; by heating (switching off) to deactivate the catalyst, network dynamics can also be thoroughly terminated regardless of the conditions of the surrounding environment, thus achieving excellent stability for error-free working. Accordingly, the authors showed the reprogramming of the one-arm bending flower actuator (mode A) into a four-arm bending flower actuator (mode B) through reswelling the actuators in the catalyst solution for switching on the dynamics of the networks (Fig. 10b). Unique to this work, the actuator in either mode A or mode B exhibited stable actuation performance and geometries for a long time because the network dynamics was switched off.

4.2 Multiple actuations realized by the shape memory effect

The shape memory effect (SME) is well known for allowing multi-cycle and fast reprogramming, which exhibits feasibility
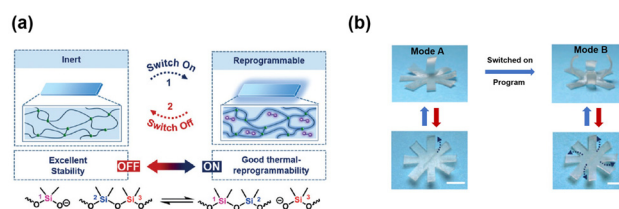

Fig. 10 (a) Illustration of switching on/off the thermal re-programmability and the anionic base-induced siloxane exchange. The purple dumbbell in the schematic illustration indicates the bis(-tetramethylammonium) oligo-dimethyl siloxanediolate (TMA-DMSiO) serving as a catalyst, and the blue lines indicate the siloxane main chains. (b) Demonstration of re-switching on the thermal re-programmability and reprogramming the one-arm bending motion into four-arm bending motion. Scale bar: 5 mm. Reproduced with permission from ref. 20. Copyright 2020 Wiley VCH.

6768 | *J. Mater. Chem. B*, 2024, **12**, 6757–6773

This journal is © The Royal Society of Chemistry 2024

to be utilized for changing the geometry and mesogen alignment of LCP actuators.[82–85] Up to date, researchers have investigated various kinds of SME in LCPs, and several inspiring works that attempted to combine the SME and reversible deformation for fabricating LCP actuators with multiple actuations have been reported recently.[86]

4.2.1. The mechanism of reprogramming based on SME. Generally, SME requires two key units including the transition unit and the fixing unit. The transition unit is responsible for the freezing and activation of chain mobility, thus memorizing the temporary shape and ensuring the recovery to the permanent shape. A series of physical phase transitions can serve as the transition units, such as glass transition, crystalline transition and so on. In most occasions, the crosslinked networks act as the fixing units, which are used to avoid the sliding of the polymer chains during the shape morphing process for the maintenance of permanent shape.

Fig. 11 demonstrates the process and mechanism of the typical dual thermo-responsive SME with the glass transition serving as the transition unit.[85] Wherein, the word "dual" means the SME exhibited two different shapes including a permanent shape and a temporary shape during the SME process.[87] At first, the sample in the permanent shape was unable to be programmed because the chain mobility was frozen. Then, the sample was heated above the temperature of glass transition (T_g) to activate the chain mobility. At this moment, the sample allowed programming by external force from the initial shape of the four-angle star to a crane. Afterwards, the sample was cooled with the load on, the temporary crane shape was memorized by freezing the chain mobility and the strain energy was stored. Finally, the sample was heated above T_g again, activating the chain mobility and releasing the stored strain energy, and the sample recovered from the temporary crane shape to the permanent shape.

4.2.2. Thermally induced shape memory effect of LCPs. Dual thermal-responsive SME widely exists in LCPs because of the crosslinked network and the glass transition unit which the LCPs intrinsically possess.[86] Additionally, the distinct isotropic transition of LCPs was also able to act as the transition unit. Mather et al. synthesized a kind of LCP material capable of keeping rubbery at the temporary shape by adopting the LC

Fig. 11 Demonstration of typical thermally induced shape memory effect. The upper parts show the sequentially changing structures and treatment during the process, and the bottom parts show the status of the chain mobility corresponding to each shape. The black round dots indicate the crosslinked points of the network, the blue lines indicate the polymer chains with the mobility frozen and the red lines indicate the polymer chains with the mobility activated.

phase as the transition unit with the T_{NI} much higher than the T_g, which was hard to achieve for the LCPs performing SME based on the glass transition or crystalline transition.[88]

Compared with dual SMEs, the triple shape memory effect (TSME) produced additional temporary shapes so that they were compatible with more diverse programming pathways and stepwise shape morphing among more intermediate shapes. The investigations of the thermal responsive TSME in LCPs mainly adhered to the strategy to create two thermal transition units with their transition temperature obviously separating, for instance, by constructing distinct glass transitions and isotropic transition or two distinct glass transitions.[89,90]

4.2.3. Light-induced shape memory effect of LCPs. Taking advantage of light as a remote stimulus that propagates directionally, the photoresponsive SME is energy efficient and offers control with high spatiotemporal resolution, capturing the researchers' attention. By far, achieving a light-responsive SME in LCPs has been mainly based on equipping the LCPs with photosensitive fillers or functional groups, wherein most investigations chose the local heating stemming from the photothermal effect as the stimulus.[91]

Surprisingly, Yu et al. innovatively created a strategy to trigger an athermal SME by utilizing the special photoswitchable T_g phenomenon based on the photochemical transition in an azobenzene-containing LCP (Azo-LCP).[92,93] As shown in Fig. 12a, the authors synthesized an Azo-LCP by ROMP, with the azobenzene moiety serving as the transition unit and the ester crosslinked network acting as the fixing unit. Unique to this work, the $T_{g-trans}$ (the T_g of Azo-LCP in which the azobenzene moieties were in trans form) was higher than the room temperature (RT) while the T_{g-cis} (the T_g of Azo-LCP in which the azobenzene moieties were in the cis form) was lower than RT, thus allowing the tunability of chain mobility via the control of isomerization of azobenzene moieties with light irradiation at constant RT. By alternative irradiation of UV light and visible light for activating or freezing the chain mobility, the Azo-LCP realized an athermal SME as shown in Fig. 12b.

Also utilizing the special photoswitchable T_g phenomenon of the azobenzene polymer network (APN), Zhu et al. developed a photo-organizable triple shape memory polymer (POTSMP) by combining this mechanism with the photothermal effect.[94] The molecular structure of the POTSMP is shown in Fig. 12c, wherein the azobenzene mesogens served as the transition unit 1 triggered by light in an athermal manner and the hydrogen bonding network formed by the urethane bonds served as the transition unit 2 triggered by light in a photothermal manner. By integrating the light-induced TSME, kirigami, origami and light-welding, a distinctive programmatic recovery process of POTSMP was realized, as shown in Fig. 12d. Firstly, under the irradiation of strong UV light, both the transition units were turned on, allowing the folded initial permanent shape (PS) to be programmed into a tubular temporary shape 1 (TS1). After cooling to RT, the transition unit 2 was turned off while the transition unit 1 was still turned on. The TS1 was further programmed into a flat temporary shape 2 (TS2) with grooves and then the irradiation of visible light turned off the transition
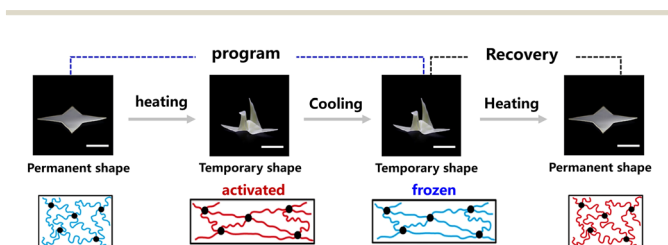
This journal is © The Royal Society of Chemistry 2024

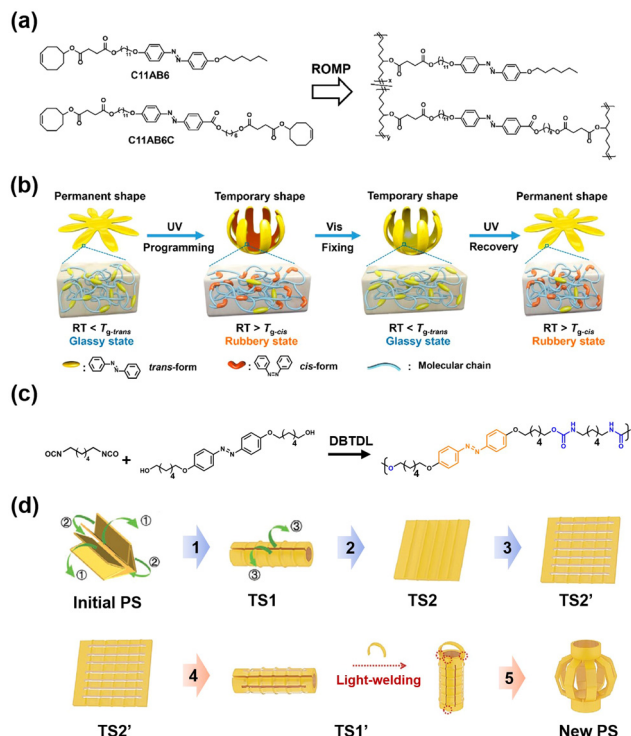*J. Mater. Chem. B*, 2024, **12**, 6757–6773 | **6769**

Fig. 12 (a) Synthesis of the APN *via* ring-opening metathesis polymerization (ROMP). (b) Shape memory effect of a modeling flower and the mechanism of the athermal shape memory effect of APN. (c) Synthetic route for POTSMP. The main components to realize triple shape memory are highlighted. (d) The photo-organizable operation for fabricating a kirigami 3D space capsule frame under light stimulation. PS: permanent shape; TS: temporary shape.

unit 1, fixing the TS2. Afterwards, the TS2 recovered to TS1′ and a new PS successively by turning on the transition unit 1 first and the transition unit 2 later. Due to the restrained shape morphing stemming from the cut out and handle processed in TS1′ by light-welding, the TS1′ recovered to the targeted 3D space capsule frame.

Inspired by the design of strain energy in the SME enabling light-induced large shape morphing, Yu *et al.* applied it in LCPs for realizing ultra-large light-induced contraction as large as 81% based on the storage and release of the strain energy, which was hard to achieve for the previously reported LCP systems that contracted based on the reversible phase transition of ordered mesogens.[95] Furthermore, they have made attempts to integrate the light-induced SME and photodeformation in the same material.[96] Through choosing the formation temperature of the crosslinking network within or outside the LC phase, selective exhibition of SME or reversible deformation in the same LCPs was achieved, providing a new photoresponsive block for the fabrication of soft actuators.

4.2.4. Reprogramming of temporary shapes for multiple actuations of LCP actuators. Recently, several inspiring works that tried to combine reversible deformation and the SME in the same monolithic LCP actuator have been reported, wherein the former was used for the actuation and the latter was responsible for reprogramming. As shown in Fig. 13a,
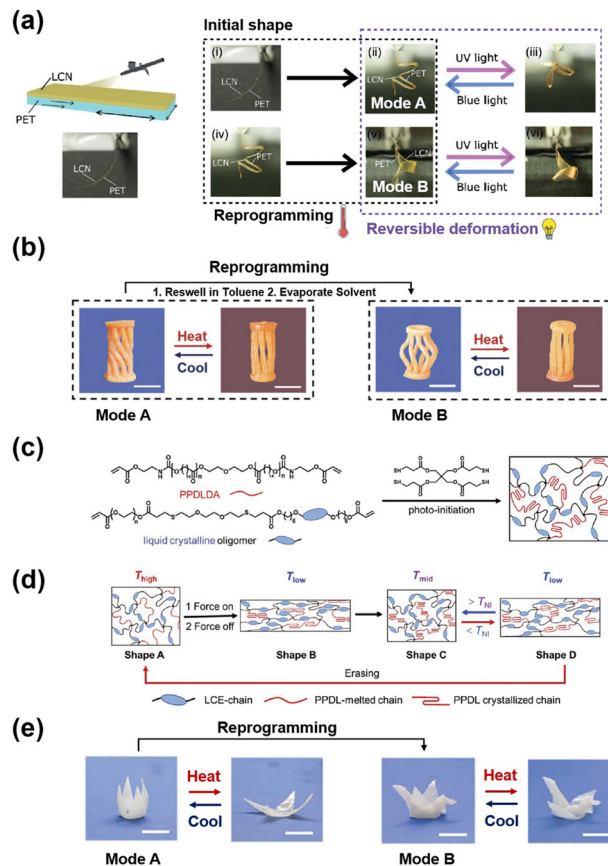

Fig. 13 (a) Schematic depiction and physical photographs of the PET/LCP bilayer, wherein the PET serves as the thermoplastic polymer and the spray-coated LCN as the light-responsive polymer. Subsequent figures show the reprogramming from the accordion-like actuator (mode A) to a spiral-like actuator (mode B), with the demonstration of their light-induced actuation. (b) Demonstration showing the change of actuation from twisting to compression by reprogramming the pillar structure from a twisted configuration (mode A) to a compressed configuration (mode B). Reproduced with permission from ref. 18. Copyright 2021 Wiley-VCH. (c) Synthetic scheme of the dual-phase LCE. (d) Schematic illustration showing the mechanism for reprogramming of mesogen alignment and geometry. (e) Demonstration of the actuation before the programming (mode A) and after the reprogramming (mode B). Reproduced with permission from ref. 97. Copyright 2022 Wiley-VCH.

Schenning *et al.* fabricated a reprogrammable light-responsive LCP actuator through spray-coating of polyethylene terephthalate (PET) with an azobenzene-doped light-responsive LCP, achieving fast reprogramming of LCP strips.[17] The bilayer strip allowed convenient and quick thermal reprogramming based on the thermoplasticity of PET from an accordion-like actuator (mode A) exhibiting origami-like bending to a spiral actuator (mode B) showing unwinding under the irradiation of UV light.

To facilitate the reprogramming of LCP actuators with complex 3D geometries based on the SME, Yang *et al.* proposed a solvent evaporation/reswelling approach. Compared with the aforementioned spray-coating methods which only operated for thin film actuators, this approach allowed reprogramming of intricate structures.[18] They utilized the micro-pores forming during the solvent evaporation process of the swollen LCP

6770 | *J. Mater. Chem. B*, 2024, **12**, 6757–6773

This journal is © The Royal Society of Chemistry 2024

sample as the transition unit. When the swollen LCP sample was deformed and subsequently evaporated in the deformed state, the orientation induced by external force and the programmed shapes were fixed by the micro-pores. Furthermore, the physically fixed mesogenic alignment and geometry were not disturbed by chain segmental (or mesogenic) movements when heated above the T_{NI}, ensuring the thermally induced actuation in the programmed temporary shape. When the dry LCP sample was swollen again, the micro-pores vanished which resulted in both the erase of alignment and the recovery of the temporary shape, thus allowing the next reprogramming. Accordingly, they reprogrammed a pillar structure from the twisted structure (mode A) to the compressed structure (mode B), with the actuation mode changing from thermally induced twisting to compression (Fig. 13b).

Furthermore, Xie et al. synthesized a dual-phase LCP network which possessed a LC phase and a crystal phase (Fig. 13c), with T_m (the temperature of crystalline melting transition) higher than T_{NI}.[97] By utilizing the crystallization phase as the transition unit for the SME, they achieved reprogramming of LCP actuators with intricate geometries in seconds. As shown in Fig. 13d, the LCP was deformed at Thigh for orienting mesogens and then cooled down to T_{low} with the load on for fixing the temporary shape ($T_{high} > T_m > T_{mid} > T_{NI} > T_{low}$). Upon heating to T_{mid}, the strain fixed by the LC phase was recovered, so the Shape B partially recovered to yield Shape C. It is worth noting that the surrounding crystals remained oriented during the process, thus serving as a build-in alignment template for the preservation of the ordered mesogen alignment. As such, reversible actuation between Shape C and Shape D occurred as the temperature switched across T_{NI}. Simple reheating above the T_m and then cooling below the T_{NI} with a different pattern of applied external force allowed reprogramming to a different geometry with another actuation mode. As shown in Fig. 13e, the LCP actuator was reprogrammed from the flower shape (mode A) to the crane shape (shape B) in seconds, with the thermal actuation mode altering from the opening and closing of the flower to the flapping of the wings of the crane, exhibiting the superiority of the dual-phase LCP enabling reprogramming of the complex structure and actuation mode in a rapid manner.

5. Summary and outlook

Deformable liquid crystal polymers perform attractive rapid reversible deformations in response to external stimuli and appear as a powerful candidate for intelligent soft actuators. In this review, the focus is placed on the fabrication method for complex actuations and the design of the reprogrammable LCPs for multiple actuations. The fabrication method plays an important role in realizing desirable complex actuations, because it determines both the mesogen alignment and the geometry of LCP actuators, which further decides the actuation mode. The reprogrammable LCP materials offer the opportunities for actuators to change their mesogen alignment and

geometry even after the shaping of their starting structures. Accordingly, actuation modes become changeable and LCP actuators with multiple actuations are achieved via reprogramming. These summaries give unprecedented insights and are used for providing a comprehensive understanding of the developing history of the fabrication methods for complex actuations and the design of reprogrammable LCP materials for multiple actuations.

LCP actuators with complex actuations perform more diverse and powerful functions compared with the ones with simple actuations, which exhibit much potential in various fields, including soft robotics, biomedical engineering, and optics. Breakthroughs of the fabrication methods are anticipated by the application of 3D printing, which allows the realization of both sophisticated bulk geometries and locally programmable stimuli-responsive properties for complex actuations. Compared with previously reported fabrication methods, relative investigations are still at the starting stage but carry considerable significance. Critical investigations, such as the universal rheology behavior of LCP inks, LCP inks responsive to a variety of stimuli beyond heat, an advanced 3D printer capable of offering even more precise control and so on, are still waiting for deeper exploration for which more research interests and efforts should be invested.

LCP actuators with multiple actuations exhibit unique advantages when it comes to carrying tasks in complex or changeful working environments towards real-world usage scenarios. Till now, researchers have successfully realized the switch of actuation modes in monolithic LCP actuators through reprogramming with intervention of external force or manual handling based on dynamic networks or shape memory effects. To facilitate the LCP actuators towards a higher intelligence level, actuators capable of continuously achieving the actuation in initial mode, the mode-switching, and subsequently the actuation in another mode through non-contact manipulation are desired. We even envision that multi-modal self-adaptive LCP actuators process internal feedback and self-regulate the actuation modes in response to the working environment. Furthermore, by integrating the self-adaptive LCP actuators with memory components which allow knowledge storage and recall, intelligent systems capable of learning from the surroundings and regulating their later behaviors accordingly may come true, thus realizing higher complexity and functionality close to that of living organisms. In our view, investigations focusing on the fabrication methods for enhancing the intelligence of LCP actuators and correlated systems, the design of novel materials consisting of multiple responsive units, and the assembly methods for integrating different functional components will be a hot topic in the future.

Regarding the development of functions, full advantages should be taken of the LCP actuators with complex and multiple actuations to realize various functions in practical applications, such as precise mechanical operation, biochemical testing, wearable devices, exploration in extreme environments, etc. The improved functions will be achieved mainly by means of bionics to investigate how living organisms learn and adapt

This journal is © The Royal Society of Chemistry 2024

J. Mater. Chem. B, 2024, **12**, 6757–6773 | **6771**

to the surrounding environment, and take inspirations from nature to design and develop novel functional LCP actuators with multiscale structures.

Author contributions

Xiaoyu Zhang: conceptualization and writing; Jia Wei: review and editing; Lang Qin: review and editing; and Yanlei Yu: funding acquisition, project administration, and review and editing.

Conflicts of interest

The authors have no competing financial interests to declare.

Acknowledgements

References

1 S. Yagai and A. Kitamura, *Chem. Soc. Rev.*, 2008, **37**, 1520–1529.

2 F. Xia and L. Jiang, *Adv. Mater.*, 2008, **20**, 2842–2858.

3 A. I. Taub, *MRS Bull.*, 2006, **31**, 336–343.

4 K. Liu, Y. Tian and L. Jiang, *Prog. Mater. Sci.*, 2013, **58**, 503–564.

5 B. Peng, X. Chen, G. Yu, F. Xu, R. Yang, Z. Yu, J. Wei, G. Zhu, L. Qin, J. Zhang, Q. Shen and Y. Yu, *Adv. Funct. Mater.*, 2023, **33**(23), 2214172.

6 S. Luo, H. Sun, S. Yan, H. Huang, W. Zhang, J. Wei and Y. Yu, *Chin. J. Appl. Chem.*, 2021, **38**, 1371–1381.

7 F. Liu and M. W. Urban, *Prog. Polym. Sci.*, 2010, **35**, 3–23.

8 F. D. Jochum and P. Theato, *Chem. Soc. Rev.*, 2013, **42**, 7468–7483.

9 G. Filipcsei, I. Csetneki, A. Szilagyi, M. Zrinyi and B. Springer-Verlag, *Oligomers Polymer Composties Molecular Imprinting*, 2007, vol. 206, pp. 137–189.

10 X. Zhao, Y. Chen, B. Peng, J. Wei and Y. Yu, *Angew. Chem., Int. Ed.*, 2023, **62**(21), e202300699.

11 J. R. Capadona, K. Shanmuganathan, D. J. Tyler, S. J. Rowan and C. Weder, *Science*, 2008, **319**, 1370–1374.

12 X. Pang, J.-A. Lv, C. Zhu, L. Qi and Y. Yu, *Adv. Mater.*, 2019, **31**(52), 1904224.

13 M. Camacho-Lopez, H. Finkelmann, P. Palffy-Muhoray and M. Shelley, *Nat. Mater.*, 2004, **3**, 307–310.

14 C. Ohm, M. Brehmer and R. Zentel, *Adv. Mater.*, 2010, **22**, 3366–3387.

15 T. Ikeda, J.-i Mamiya and Y. Yu, *Angew. Chem., Int. Ed.*, 2007, **46**, 506–528.

16 M. Chen, M. Gao, L. Bai, H. Zheng, H. J. Qi and K. Zhou, *Adv. Mater.*, 2023, **35**(23), 2209566.

17 R. Verpaalen, M. Pilz da Cunha, T. A. P. Engels, M. G. Debije and A. Schenning, *Angew. Chem., Int. Ed.*, 2020, **59**, 4532–4536.

18 B. Jin, J. Liu, Y. Shi, G. Chen, Q. Zhao and S. Yang, *Adv. Mater.*, 2022, **34**(5), 2107855.

19 N. Zheng and T. Xie, *Acta Polym. Sin.*, 2017, 1715–1724, DOI: **10.11777/j.issn1000-3304.2017.17161**.

20 Y. Wu, Y. Yang, X. Qian, Q. Chen, Y. Wei and Y. Ji, *Angew. Chem., Int. Ed.*, 2020, **59**, 4778–4784.

21 Y. Yu, M. Nakano and T. Ikeda, *Nature*, 2003, **425**, 145.

22 M. Winkler, A. Kaiser, S. Krause, H. Finkelmann and A. Schmidt, *Larnaca, CYPRUS*, 2008.

23 T. Ware, M. McConney, J. Wie, V. Tondiglia and T. White, *Science*, 2015, **347**, 982–984.

24 K. Urayama, S. Honda and T. Takigawa, *Macromolecules*, 2006, **39**, 1943–1949.

25 W. Lehmann, H. Skupin, C. Tolksdorf, E. Gebhard, R. Zentel, P. Kruger, M. Losche and F. Kremer, *Nature*, 2001, **410**, 447–450.

26 J. Campos, F. Stricker, K. Clark, M. Park, S. Bailey, A. Kuenstler, R. Hayward and J. de Alaniz, *Angew. Chem., Int. Ed.*, 2023, **62**(1), e202214339.

27 A. Kaiser, M. Winkler, S. Krause, H. Finkelmann and A. Schmidt, *J. Mater. Chem.*, 2009, **19**, 538–543.

28 K. Harris, C. Bastiaansen, J. Lub and D. Broer, *Nano Lett.*, 2005, **5**, 1857–1860.

29 H. Finkelmann, E. Nishikawa, G. G. Pereira and M. Warner, *Phys. Rev. Lett.*, 2001, **87**(1), 015501.

30 D. Broer, C. Bastiaansen, M. Debije and A. Schenning, *Angew. Chem., Int. Ed.*, 2012, **51**, 7102–7109.

31 X. Huang, X. Pang, L. Qin and Y. Yu, *Acta Polym. Sin.*, 2022, **53**, 1324–1331.

32 Y. Chen, Q. Liu, P. Theato, J. Wei and Y. Yu, *Adv. Intelligent Systems*, 2021, **3**(10), 2000254.

33 Y. Feng, J. Wei, L. Qin and Y. Yu, *Soft Matter*, 2023, **19**, 999–1007.

34 D. Broer, R. Gossink and R. Hikmet, *Angew. Makromol. Chem.*, 1990, **183**, 45–66.

35 C. Yakacki, M. Saed, D. Nair, T. Gong, S. Reed and C. Bowman, *RSC Adv.*, 2015, **5**, 18997–19001.

36 H. Shahsavan, A. Aghakhani, H. Zeng, Y. Guo, Z. Davidson, A. Priimagi and M. Sitti, *Proc. Natl. Acad. Sci. U. S. A.*, 2020, **117**, 5125–5133.

37 T. Hebner, H. Fowler, K. Herbert, N. Skillin, C. Bowman and T. White, *Macromolecules*, 2021, **54**, 11074–11082.

38 D. Broer, J. Boven, G. Mol and G. Challa, *Makromol. Chem.*, 1989, **190**, 2255–2268.

39 C. Chang, C. Bastiaansen, D. Broer and H. Kuo, *Adv. Funct. Mater.*, 2012, **22**, 2855–2859.

40 M. Kondo, M. Sugimoto, M. Yamada, Y. Naka, J. Mamiya, M. Kinoshita, A. Shishido, Y. Yu and T. Ikeda, *J. Mater. Chem.*, 2010, **20**, 117–122.

41 M. Li, P. Keller, B. Li, X. Wang and M. Brunet, *Adv. Mater.*, 2003, **15**, 569–572.

42 D. Liu, C. Bastiaansen, J. den Toonder and D. Broer, *Angew. Chem., Int. Ed.*, 2012, **51**, 892–896.

6772 | *J. Mater. Chem. B*, 2024, **12**, 6757–6773

This journal is © The Royal Society of Chemistry 2024

43 Y. Yu, T. Maeda, J. Mamiya and T. Ikeda, *Angew. Chem., Int. Ed.*, 2007, **46**, 881–883.

44 Y. Yu, M. Nakano and T. Ikeda, *Pure Appl. Chem.*, 2004, **76**, 1467–1477.

45 S. Iamsaard, S. Asshoff, B. Matt, T. Kudernac, J. Cornelissen, S. Fletcher and N. Katsonis, *Nat. Chem.*, 2014, **6**, 229–235.

46 A. Gelebart, D. Mulder, M. Varga, A. Konya, G. Vantomme, E. Meijer, R. Selinger and D. Broer, *Nature*, 2017, **546**, 632–636.

47 L. de Haan, C. Sanchez-Somolinos, C. Bastiaansen, A. Schenning and D. Broer, *Angew. Chem., Int. Ed.*, 2012, **51**, 12469–12472.

48 M. McConney, A. Martinez, V. Tondiglia, K. Lee, D. Langley, I. Smalyukh and T. White, *Adv. Mater.*, 2013, **25**, 5880–5885.

49 X. Cheng and Y. Zhang, *Adv. Mater.*, 2019, **31**(36), 1901895.

50 L. de Haan, C. Sánchez-Somolinos, C. Bastiaansen, A. Schenning and D. Broer, *Angew. Chem., Int. Ed.*, 2012, **51**, 12469–12472.

51 A. Buguin, M. Li, P. Silberzan, B. Ladoux and P. Keller, *J. Am. Chem. Soc.*, 2006, **128**, 1088–1089.

52 Y. Wang, J. Liu and S. Yang, *Appl. Phys. Rev.*, 2022, **9**(1), 011301.

53 M. Ilami, H. Bagheri, R. Ahmed, E. O. Skowronek and H. Marvi, *Adv. Mater.*, 2021, **33**(19), 2003139.

54 H. Yang, A. Buguin, J. Taulemesse, K. Kaneko, S. Méry, A. Bergeret and P. Keller, *J. Am. Chem. Soc.*, 2009, **131**, 15000–15004.

55 J.-A. Lv, Y. Liu, J. Wei, E. Chen, L. Qin and Y. Yu, *Nature*, 2016, **537**, 179–184.

56 B. Xu, C. Zhu, L. Qin, J. Wei and Y. Yu, *Small*, 2019, **15**(24), 1901847.

57 S. Han, Y. Chen, B. Xu, J. Wei and Y. Yu, *Chin. J. Polym. Sci.*, 2020, **38**, 806–813.

58 Y. Lu, L. Qin, Q. Liu, Z. Li, W. Zhang, C. Zhu and Y. Yu, *NPG Asia Mater.*, 2022, **14**(1), 73.

59 Q. Liu, G. Yu, C. Zhu, B. Peng, R. Li, T. Yi and Y. Yu, *Small Methods*, 2021, **5**(12), 2100969.

60 Q. Liu, Y. Liu, J. Lv, E. Chen and Y. Yu, *Adv. Intelligent Systems*, 2019, **1**(6), 1900060.

61 H. Zeng, P. Wasylczyk, C. Parmeggiani, D. Martella, M. Burresi and D. Wiersma, *Adv. Mater.*, 2015, **27**(26), 3883–3887.

62 C. Ambulo, J. Burroughs, J. Boothby, H. Kim, M. Shankar and T. Ware, *ACS Appl. Mater. Interfaces*, 2017, **9**, 37332–37339.

63 M. del Pozo, C. Delaney, C. Bastiaansen, D. Diamond, A. Schenning and L. Florea, *ACS Nano*, 2020, **14**, 9832–9839.

64 N. Traugutt, D. Mistry, C. Luo, K. Yu, Q. Ge and C. Yakacki, *Adv. Mater.*, 2020, **32**(28), 2000797.

65 X. Peng, X. Kuang, D. Roach, Y. Wang, C. Hamel, C. Lu and H. Qi, *Additive Manuf.*, 2021, **40**, 101911.

66 D. Roach, X. Sun, X. Peng, F. Demoly, K. Zhou and H. Qi, *Adv. Funct. Mater.*, 2022, **32**(36), 2203236.

67 A. Kotikian, R. Truby, J. Boley, T. White and J. Lewis, *Adv. Mater.*, 2018, **30**(10), 1706164.

68 M. Lopez-Valdeolivas, D. Liu, D. Broer and C. Sanchez-Somolinos, *Macromol. Rapid Commun.*, 2018, **39**(5), 1700710.

69 X. Peng, S. Wu, X. Sun, L. Yue, S. Montgomery, F. Demoly, K. Zhou, R. Zhao and H. Qi, *Adv. Mater.*, 2022, **34**(39), 2204890.

70 A. Kotikian, C. McMahan, E. Davidson, J. Muhammad, R. Weeks, C. Daraio and J. Lewis, *Sci. Rob.*, 2019, **4**(33), eaax7044.

71 Z. Wang, Z. Wang, Y. Zheng, Q. He, Y. Wang and S. Cai, *Sci. Adv.*, 2020, **6**(39), eabc0034.

72 Y. Yao, J. Waters, A. Shneidman, J. Cui, X. Wang, N. Mandsberg, S. Li, A. Balazs and J. Aizenberg, *Proc. Natl. Acad. Sci. U. S. A.*, 2018, **115**, 12950–12955.

73 S. Li, M. Lerch, J. Waters, B. Deng, R. Martens, Y. Yao, D. Kim, K. Bertoldi, A. Grinthal, A. Balazs and J. Aizenberg, *Nature*, 2022, **605**, 76–83.

74 Q. Chen, Y. Yang, Y. Wei and Y. Ji, *Acta Polym. Sin.*, 2019, **50**, 451–468.

75 Z. Pei, Y. Yang, Q. Chen, E. Terentjev, Y. Wei and Y. Ji, *Nat. Mater.*, 2014, **13**, 36–41.

76 T. Ube, K. Kawasaki and T. Ikeda, *Adv. Mater.*, 2016, **28**, 8212–8217.

77 Z. Jiang, Y. Xiao, L. Yin, L. Han and Y. Zhao, *Angew. Chem., Int. Ed.*, 2020, 59, 4925–4931.

78 Z. Wen, M. McBride, X. Zhang, X. Han, A. Martinez, R. Shao, C. Zhu, R. Visvanathan, N. Clark, Y. Wang, K. Yang and C. Bowman, *Macromolecules*, 2018, **51**, 5812–5819.

79 M. Saed, A. Gablier and E. Terentjev, *Adv. Funct. Mater.*, 2020, **30**(3), 1906458.

80 M. McBride, A. Martinez, L. Cox, M. Alim, K. Childress, M. Beiswinger, M. Podgorski, B. Worrell, J. Killgore and C. Bowman, *Sci. Adv.*, 2018, **4**(8), eaat4634.

81 Z. Jiang, Y. Xiao, X. Tong and Y. Zhao, *Angew. Chem., Int. Ed.*, 2019, **58**, 5332–5337.

82 R. Zhao, T. Zhao, X. Jiang, X. Liu, D. Shi, C. Liu, S. Yang and E. Chen, *Adv. Mater.*, 2017, **29**(12), 1605908.

83 W. Peng, G. Zhang, Q. Zhao and T. Xie, *Adv. Mater.*, 2021, **33**(34), 2102473.

84 Q. Zhao, W. Zou, Y. Luo and T. Xie, *Sci. Adv.*, 2016, **2**(1), e1501297.

85 B. Jin, H. Song, R. Jiang, J. Song, Q. Zhao and T. Xie, *Sci. Adv.*, 2018, **4**(1), eaao3865.

86 R. Sun, X. Li, J. Xie and G. Hou, *China Plastics*, 2016, **30**, 1–6.

87 Q. Zhao, H. J. Qi and T. Xie, *Prog. Polym. Sci.*, 2015, **49–50**, 79–120.

88 I. Rousseau and P. Mather, *J. Am. Chem. Soc.*, 2003, **125**, 15300.

89 S. Ahn and R. Kasi, *Adv. Funct. Mater.*, 2011, **21**, 4543–4549.

90 D. Hoekstra, M. Debije and A. Schenning, *Macromolecules*, 2021, **54**, 5410–5416.

91 D. Iqbal and M. Samiullah, *Materials*, 2013, **6**, 116–142.

92 X. Zhang, C. Zhu, B. Xu, L. Qin, J. Wei and Y. Yu, *ACS Appl. Mater. Interfaces*, 2019, **11**, 46212–46218.

93 X. Zhang, L. Qin, Y. Liu, J. Wei and Y. Yu, *Giant*, 2020, **2**, 100019.

94 J. Sun, B. Peng, Y. Lu, X. Zhang, J. Wei, C. Zhu and Y. Yu, *Small*, 2022, **18**(9), 2106443.

95 X. Pang, L. Qin, B. Xu, Q. Liu and Y. Yu, *Adv. Funct. Mater.*, 2020, **30**, 2002451.

96 X. Huang, L. Qin, J. Wang, X. Zhang, B. Peng and Y. Yu, *Adv. Funct. Mater.*, 2022, **32**(51), 2208312.

97 G. Chen, B. Jin, Y. Shi, Q. Zhao, Y. Shen and T. Xie, *Adv. Mater.*, 2022, **34**(21), 2201679.

This journal is © The Royal Society of Chemistry 2024

J. Mater. Chem. B, 2024, **12**, 6757–6773 | **6773**